DNA methylation-based forensic age estimation in human bone

Shyamalika Gopalan[1], Jonathan Gaige[1], Brenna M. Henn[1,2,3]

[1]Department of Ecology and Evolution, Stony Brook University, Stony Brook, NY 11794, USA.
[2]Department of Anthropology, University of California, Davis, CA 95616, USA.
[3]UC Davis Genome Center, University of California, Davis, CA 95616, USA.

Abstract

DNA methylation is an epigenetic modification of cytosine nucleotides that represents a promising suite of aging markers with broad potential applications. In particular, determining an individual's age from their skeletal remains is an enduring problem in the field of forensic anthropology, and one that epigenetic markers are particularly well-suited to address. However, all DNA methylation-based age prediction methods published so far focus on tissues other than bone. While high accuracy has been achieved for saliva, blood and sperm, which are easily accessible in living individuals, the highly tissue-specific nature of DNA methylation patterns means that age prediction models trained on these particular tissues may not be directly applicable to other tissues. Bone is a prime target for the development of DNA methylation-based forensic identification tools as skeletal remains are often recoverable for years post-mortem, and well after soft tissues have decomposed. In this study, we generate genome-wide DNA methylation data from 32 individual bone samples. We analyze this new dataset alongside published data from 133 additional bone donors, both living and deceased. We perform an epigenome-wide association study on this combined dataset to identify 108 sites of DNA methylation that show a significant relationship with age (FDR < 0.05). We also develop an age-prediction model using lasso regression that produces highly accurate estimates of age from bone spanning an age range of 49-112 years. Our study demonstrates that DNA methylation levels at specific CpG sites can serve as powerful markers of aging, and can yield more accurate predictions of chronological age in human adults than morphometric markers.

Introduction

Determining a person's age from skeletal and dental remains has been an integral component of building a biological profile for several decades of forensic investigations. Classic methods rely on morphological features of development and functional decline, such a tooth eruption, suture closure, and bone density (Cunha et al., 2009; Franklin, 2010). However, these approaches suffer from difficulties in implementation and standardization (Cunha et al., 2009; Franklin, 2010). One such issue is that there are few morphological features that can be used to precisely estimate the age of adults, as most developmental processes that can distinguish between juveniles of different ages cease by adulthood. Thus, different skeletal features are analyzed for this purpose in different age classes, but the overall accuracy of morphology-based estimates is typically low for adults (Cunha et al., 2009; Franklin, 2010).

Molecular-based methods of age estimation represent a promising alternative to those based on morphometrics. One early approach was based on the degree of amino-acid racemization of bones and teeth, which produces highly accurate estimates of age (Meissner and Ritz-Timme, 2010; Ohtani and Yamamoto, 2010). However, this method still suffers from practical limitations, such as difficulties in standardizing the procedure, and the need for specialized equipment and technical expertise to isolate the tissue of interest and conduct protein fractionation (Meissner and Ritz-Timme, 2010; Ohtani and Yamamoto, 2010).

More recently, advances in the study of DNA methylation have driven its popularity in the field of forensic sciences as a general molecular approach to estimating individual age that can be applied in various contexts. DNA methylation is a chemical modification to the primary DNA sequence; in mammals, it occurs predominantly on cytosine nucleotides that are in a cytosine-guanine dinucleotide context (a CpG site). It has been shown that, at certain CpG sites, the average level of DNA methylation changes measurably throughout life in a manner that makes them potentially useful markers of human aging. This has led to a profusion of methods being developed for tissues such as sperm, blood, saliva, and teeth which produce highly accurate estimates based on DNA methylation levels from relatively few CpG sites, measured using widely used, often commercially available, assay methods (Hong et al., 2017; Lee et al.,

2015; Vidaki et al., 2017; Yi et al., 2014; Zbieć-Piekarska et al., 2015b). However, there does not yet exist a DNA methylation-based method for estimating age from human bone, a tissue type that is highly relevant to the field of forensic sciences. Methods developed for other tissues likely cannot be applied directly to bone due to the highly tissue-specific nature of age-related DNA methylation patterns (Dmitrijeva et al., 2018; Hannum et al., 2013; Lee et al., 2015; Maegawa et al., 2010; Slieker et al., 2018).

In this study, we analyze bone-derived DNA methylation data from hundreds of thousands of CpG sites across the genome in a large sample of human adults to identify CpG sites that change significantly with age. We then use a subset of these sites to develop a highly accurate prediction model for individuals in an age class where morphological methods can be problematic. Furthermore, we show that our model exhibits higher accuracy and relies on fewer CpG sites compared to a previously published model that was developed for use on multiple tissues.

Methods

Description of datasets

Three previously analyzed and published datasets were derived from bone biopsies of living donors, assayed on the Illumina Human Methylation 450k array, and previously analyzed (Table 1) (Horvath et al., 2015; Reppe et al., 2017). Additional data were generated for this study from bone-derived DNA from deceased donors from both forensic and preserved specimens and assayed on the Illumina Human Methylation EPIC array (Table 1).

81 Table 1 - Description of datasets analyzed.

82

Dataset (GEO accession)	**N samples**	**N females**	**Age range**	**Sample type**	**Methylation array**	**Citation**
Osteoporosis study	84	84	49-86	Living donor	450k	(Reppe et al., 2017)
Multi-tissue study (GSE64490)	48	46	49-104	Living donor	450k	(Horvath et al., 2015)
Supercentenarian from multi-tissue study (GSE64491)	1 (plus 3 replicates)	1	112	Deceased donor	450k	(Horvath et al., 2015)
Preserved specimens	19	7	60-97	Deceased donor	EPIC	This study
Forensic specimens	13	4	18-95	Deceased donor	EPIC	This study

83

Forensic specimens

Forensic specimens were collected from the Forensic Anthropology Center at Texas State (FACTS) in San Marcos, Texas. Donated specimens are typically allowed to decompose naturally in an outdoor environment on the premises for 2-3 years, after which the bones are cleaned with a mild detergent and housed in their storage facilities. For this study, trabecular bone from femurs was collected based on a previously published protocol for minimally destructive sampling for skeletal remains (Gibbon et al., 2009). Briefly, the outside of the bone was cleaned between the medial and lateral condyles with 95% ethanol. The femur was then held vertically while a small hole was drilled with a Dremel 200 rotary tool and a 1/8" diameter bit. After rotating the fully inserted drill bit and withdrawing it, the femur was inverted over a collection tube to collect the bone powder. Between 0.1 and 1g (0.67g average) of bone powder was recovered for these samples.

Preserved specimens

Preserved specimens were collected from the Department of Anatomical Sciences Stony Brook University. Bodies donated to this facility are treated with chemical preservatives and used in medical and dental anatomy courses. For each sample, a Dremel 200 rotary tool with a 1" cutting disc was used to extract a piece of tissue that contained the petrous portion of the temporal bone, which has been previously shown to be among the densest skeletal elements in the body and typically contains relatively uncontaminated endogenous DNA in even ancient samples (Pinhasi et al., 2015). This piece was then pre-digested in a solution of TE buffer and proteinase K at 55°C for up to 5 days, or until all soft tissue was dissolved, leaving behind only bone. This piece was then subsampled into smaller pieces and ground to a fine powder using a combination of a mortar and pestle and an IKA tube mill. Between 0.27 and 1.13g (0.54g average) of bone power per sample was extracted.

DNA extraction

Bone samples underwent a pre-digestion step prior to DNA extraction using a standard phenol-chloroform method. The powder was incubated in a solution of 250 uL of N-

Laurylsarcosine and 30uL proteinase K in 10mL EDTA at 55°C on a nutating mixer for two days to dissolve the mineral structure of the bone. If powder was not completely dissolved after two days, an additional 5mL of EDTA was added and the sample incubated for a further two days. One volume of phenol-chloroform was then added to the dissolved bone solution, shaken at room temperature for one minute, and centrifuged for 20 minutes at 3,500 rpm. The aqueous phase was transferred to a fresh tube where one volume (the same amount as EDTA and phenol-chloroform) of chloroform was added. The sample was again shaken for one minute and centrifuged for 20 minutes. The aqueous phase was then transferred to an Amicon Ultra-15 filter and centrifuged for up to 20 minutes, or until most of the liquid passed through. The filter was washed with 12mL of ultra-pure HPLC water and spun down until most of the liquid passed through. If necessary, this step was repeated until the wash-through liquid was clear.

Methylation array data processing and quality control

DNA methylation data generated for this study was preprocessed from raw intensity files (IDATs) using the R package minfi (Aryee et al., 2014). The GEO deposited datasets were preprocessed from raw methylated and unmethylated counts using the R packages lumi and methylumi (Davis et al., 2015; Du et al., 2008). Raw data was not available for the osteoporosis study, so pre-processed and rescaled data (by beta mixture quantile dilation – BMIQ) provided by the author was used (Reppe et al., 2017). All raw data were first filtered for poorly performing samples and CpG sites. Samples were flagged if their median methylated or unmethylated levels were low (if log2 of the count was less than 10.5), if more than 10% of measured probes exceeded a detection p-value threshold of 1%, or if the sex predicted by X and Y chromosome methylation levels did not match the reported sex, as per standard DNA methylation array processing procedures (Aryee et al., 2014). All forensic samples failed these quality control measures. Probes that were among previously identified cross-reactive probes were removed (Chen et al., 2013; Pidsley et al., 2016). Colour correction, background correction, and functional normalization of IDAT data was conducted with the 'preprocessFunnorm' function in minfi (Aryee et al., 2014). Colour correction, background correction, and shift and scaling normalization of signal count data was conducted with the

'lumiMethyC' and 'lumiMethyN' functions in lumi (Du et al., 2008). Rescaling of type 1 and 2 probes was conducted by BMIQ, implemented in the R package wateRmelon. All remaining probes that failed a detection p-value threshold of 5% were then set to NA and all CpG sites on sex chromosomes were also removed. Continuous beta values for each CpG site, which range from 0 (indicating that the site is completely unmethylated) to 1 (completely methylated), were extracted for subsequent analysis.

Principal components analyses

We conducted a principal components analyses (PCA) on the merged dataset of samples that were successfully assayed (n = 155) in order to identify factors correlated with significant sources of variation across the datasets. PCAs were conducted with the 'prcomp' function in R.

Epigenome-wide association study (EWAS)

An EWAS for age was performed using the R package CpGassoc on the combined dataset of 155 individuals and all CpG sites that were present on the 450k dataset and passed quality control. Dataset identity was included as a covariate to control for excessive genomic inflation in the EWAS.

Horvath age prediction

The original Horvath age prediction algorithm was implemented by using the 'agep' function from the R package wateRmelon on the preprocessed and normalized data (Horvath, 2013; Pidsley et al., 2013). The optional normalization step in the Horvath workflow was not used.

Developing age prediction models

We created a training set of data to develop an age prediction model by randomly sampling approximately 70% of individuals from each dataset, except for GSE64491, which contains four replicates of one individual; these were evenly divided into the test and training dataset. We then made minor label adjustments to ensure that the training set always

contained the widest possible age range. We then used lasso regression, implemented in the R package glmnet (Friedman et al., 2010), to select predictors from only those CpG sites that were found to be significantly associated with age (FDR < 0.05) in the EWAS. We varied the regularization penalty parameter (λ – not to be confused with the genomic inflation factor) across a range to select two primary models: the best model had the lowest prediction error in the training dataset, and the other model had a prediction error within one standard error of the minimum in the training dataset.

Gene region enrichment analysis

The 37 CpG sites comprising the best performing model were tested for enrichment of several possible categories, including gene and disease ontology terms, phenotypes, genes, and Molecular Signatures Database (MSigDB) terms using Genomic Regions Enrichment of Annotation Tool (GREAT) (McLean et al., 2010). A custom background set of all CpGs tested in the EWAS was used.

Results

Data quality

Genome-wide methylation data was successfully generated for all preserved specimens, but all forensic samples failed post-assay quality control measures. For the latter, both median methylated and unmethylated signals were too low to pass the threshold and all samples had a high proportion of unreliable probes (see *Methods*). Furthermore, while the median methylated signal was significantly lower than the median unmethylated signal across all samples ($p = 9.2 \times 10\text{-}6$, paired sample t-test), this difference was more pronounced in the forensic samples ($p = 4.1 \times 10\text{-}14$, t-test) (Figure 1). The forensic samples were excluded from all subsequent analyses.

Principal components analysis

198 A principal components analysis of the 155 successfully assayed samples showed that
199 batch effects were the major drivers of the first two principal components, which together
200 accounted for over 55% of the variation in the dataset (Figure 2).
201
202 *Epigenome-wide association study (EWAS)*
203 We performed an EWAS on the merged DNA methylation dataset to identify CpG sites
204 that were significantly associated with age in bone tissue (see *Methods*). When not correcting
205 for dataset identity, we observed extreme genomic inflation, which is not unexpected given the
206 substantial batch effects observed and the differences in age distributions across the three
207 largest datasets (Figures 2-3; Table 1). When using dataset identity as a covariate in the EWAS,
208 this inflation was greatly reduced, and 108 CpG sites were significantly associated with age (FDR
209 < 0.05) (Figures 3-4).
210
211 *Developing and evaluating models for chronological age prediction for bone*
212 We used the prediction model published by Horvath (2013), which leverages DNA
213 methylation information from 353 CpG sites, to estimate the age of the individuals in the
214 merged dataset. The model was trained on DNA methylation data derived from 13 different
215 tissue types, including bone marrow, but not hard bone tissue (i.e. osteocytes and osteoblasts)
216 (Horvath 2013). It was previously tested on the bone samples from the GSE64490 and
217 GSE64491 datasets in Horvath et al. 2015 (see Figure 6 in that paper) and was consequently
218 described as also being applicable to hard bone tissues, although no metric of accuracy was
219 reported (Horvath et al 2015). We visually parsed 51 of the 52 data points in the GSE64490 and
220 GSE64491 datasets using a plot digitizer (Rohatgi, 2018), and estimated the root mean squared
221 error (RMSE) to be 8.1 years. Our application of the same model to these datasets, appears to
222 have yielded more accurate results than the initial publication (5.9 and 6.3 years, respectively,
223 and 6.0 across both datasets; Figure 5). The reasons for this are unclear, but could be attributed
224 to differences in how the data were processed prior to running the age prediction algorithm
225 (see *Methods* and *Discussion*).

We sought to determine if accurate estimates of individual age could be achieved for human bone using fewer than 353 sites. We split the individuals in the datasets into training and test groups and used lasso regression to select predictor variables from among the 108 age-associated CpGs identified in the EWAS (see *Methods*). The model that minimized the prediction error in the training data was based on information from 46 sites, while a second model exhibited comparably low error using information from only 37 CpG sites. Both models included two CpG sites that are also used in the Horvath model. These two new models were also used to generate estimates of age for all individuals in the dataset, and the RMSE between the true age and the prediction in the test dataset was calculated (Table 2). Both models were more accurate than the Horvath model, with the sparser model (based on 37 CpG sites) being slightly more accurate in the test samples overall (Figure 5; Table 2). This model is hereafter referred to as the 'bone clock', and additional details for the specific CpG sites that comprise it are given in Table 3.

An enrichment analysis identified two significant categories as being overrepresented in these 37 bone clock CpG regions; the gene ELOVL2 was represented twice (a 948-fold enrichment relative to the background, p = 2.1 x 10-6), and genes bearing the motif 'AAGCACA' in their 3' untranslated regions (UTRs) were represented 8 times (4.8-fold enrichment, p = 2. 1 x 10-4).

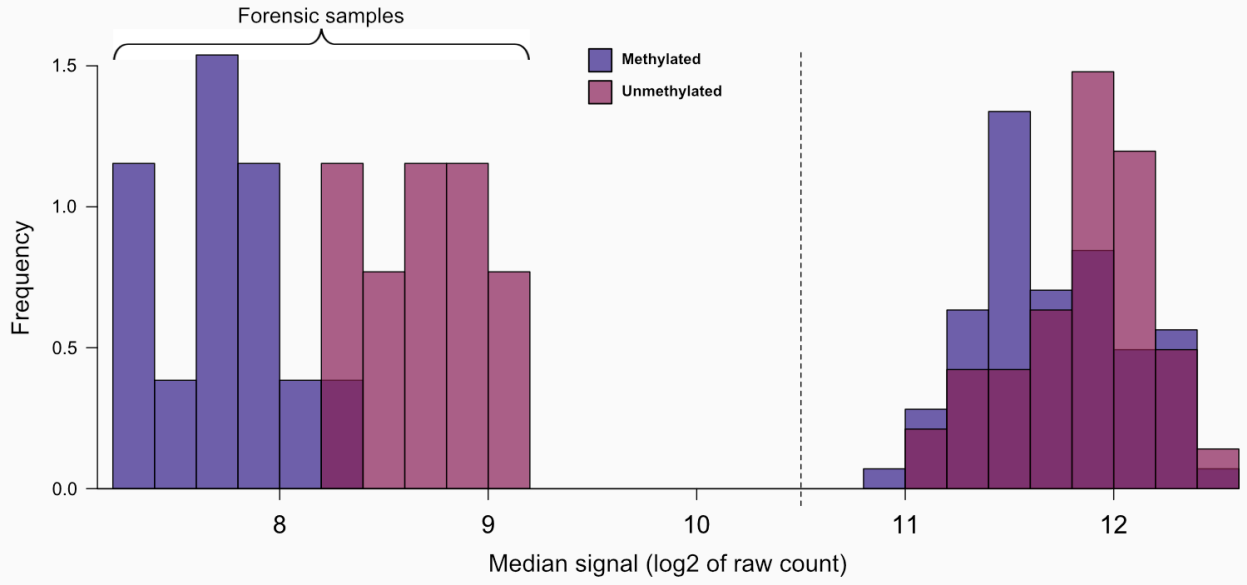

Figure 1 - The distribution of median methylated (blue) and unmethylated (red) signal values in forensic samples (left) and all other samples (right). The threshold typically used for post-assay quality control is indicated with the dashed line (Aryee et al., 2014). All forensic samples in this study failed to meet this threshold and were thus excluded from subsequent analysis.

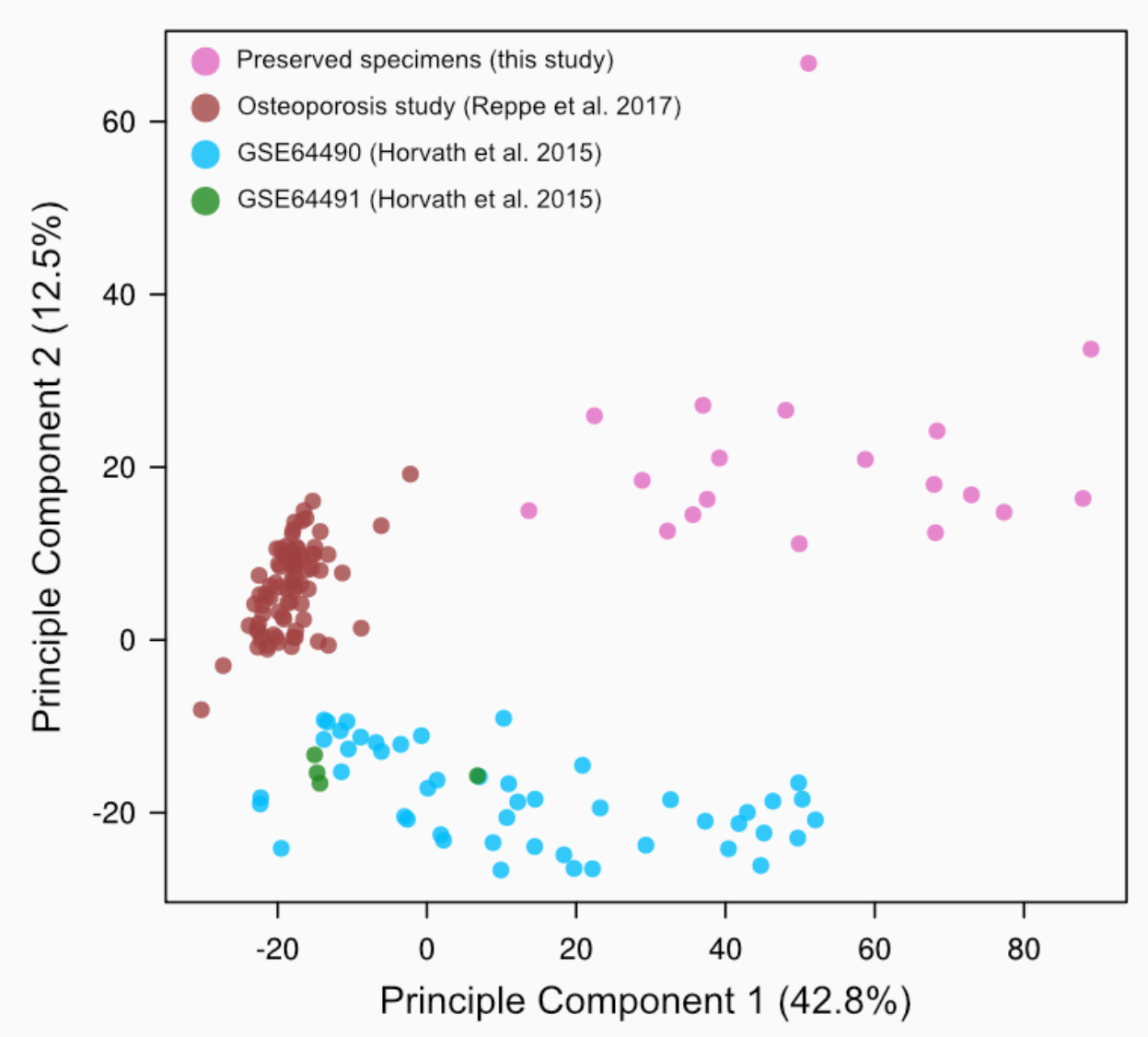

Figure 2 - Scatterplot of the first two principal components of variation in the DNA methylation dataset.

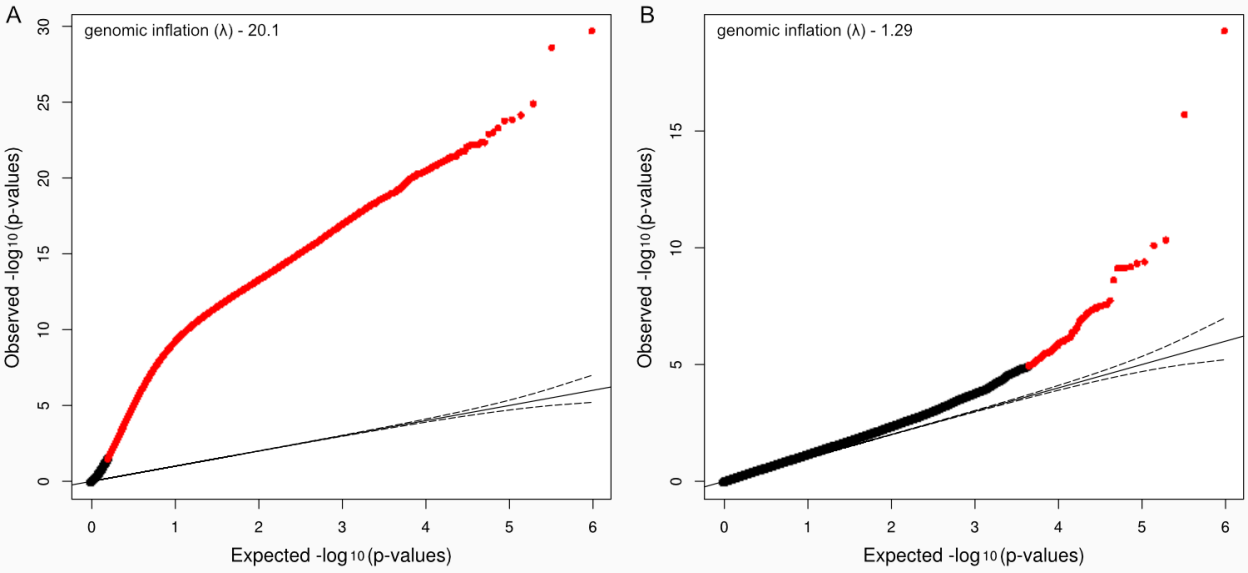

Figure 3 - Quantile-quantile plot of expected p-values (under a uniform distribution) versus observed p-values in the EWAS. The points represent p-values for a tested CpG site. Red points indicate those that are found to be significantly associated with age (FDR < 0.05). A) When no covariates are used, an excessive number of CpG sites are found to be significant. B) The inclusion of dataset identity appears to correct this, likely by accounting for batch effects between sets of samples that were assayed separately.

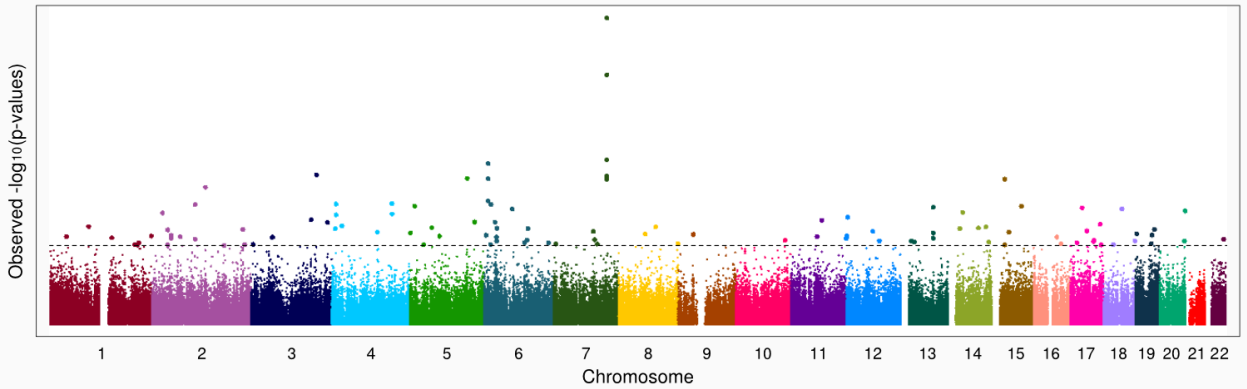

Figure 4 - Manhattan plot depicting the location of all CpG sites tested in the EWAS where dataset identity was included as a covariate. The false discovery rate threshold of 0.05 is indicated by the horizontal dashed line. 108 CpG sites were found to exceed this threshold (larger dots).

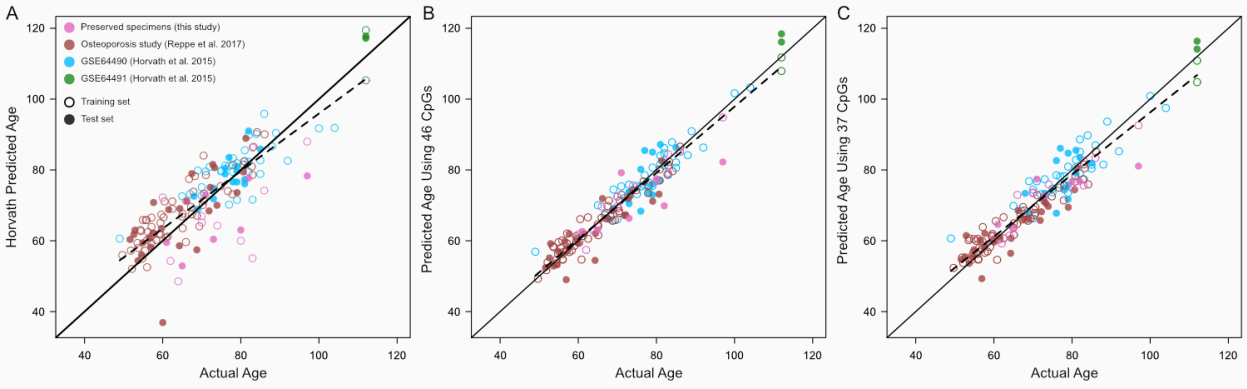

Figure 5 - True chronological age versus estimates from three DNA methylation-based models. A) Age estimates from A) the Horvath model, based on DNA methylation data from 353 CpG sites, B) the 46-site model and C) the 37-site model. Outlined circles represent samples that were used to train the 46- and 37-site models, while solid circles represent test set samples.

279 Table 2 - Root mean squared errors (RMSE) for each prediction model tested; the Horvath
280 model, the 46-site model and the 37-site model. As the Horvath model was not trained on any
281 of the individuals analyzed here, the RMSE for all samples is also reported. Of these three, the
282 37-site bone clock performs best in the test set of individuals.
283

	Root mean squared error (years)					
		Test samples				
Model	*All samples*	All test samples	Preserved samples (this study)	Osteoporosis study (Reppe et al. 2017)	GSE64490 (Horvath et al. 2015)	GSE64491 (Horvath et al. 2015)
Horvath model	7.4	7.7	11.7	8.1	3.9	5.5
46 site model	-	5.1	8.4	4.2	4.6	5.4
37 site model	-	4.9	7.1	4.2	4.8	4.3

284
285

286 Table 3 – Details of the 37 bone clock CpG sites. The names of all CpG sites that comprise our
287 best model are reported here, along with their genomic positions (based on the hg19/GRCh37
288 reference), the gene(s) they are annotated to (if any), and their relative positions within those
289 genes. The positions of these CpG sites are either within the transcriptional start site (TSS),
290 gene body, exons, or untranslated regions (UTR). The two bone clock CpG sites that are also
291 used by the Horvath clock are indicated by an asterisk.
292

Name	Position	UCSC Gene Name	UCSC Gene Group
cg01974375	1:151298954	PI4KB	TSS1500
cg21748207	2:26395359	FAM59B	TSS1500
cg12206199	2:39187543	LOC375196, LOC100271715	TSS200, Body
cg20547295	2:69664869	NFU1	TSS200
cg27213509	2:176947228	EVX2	Body
cg21545859	3:5068037		
cg03607117	3:53080440	SFMBT1	TSS1500
cg07553761	3:160167977	TRIM59	TSS1500
cg23995914	4:10459228	ZNF518B	TSS200
cg07171111	4:10462903		
cg01899437	4:24914441	CCDC149	1st exon, 5'UTR
cg03133735	4:111562270		
cg03663715	5:72744904	FOXD1	TSS1500
cg23500537	5:140419819		
cg13773570	6:6006707	NRN1	Body
cg16867657	6:11044877	ELOVL2	TSS1500
cg24724428	6:11044888	ELOVL2	TSS1500
cg00464814	6:16758889	ATXN1	5'UTR
cg22736354*	6:18122719	NHLRC1	1st exon
cg10970124	6:31634602	BAT4, CSNK2B	TSS1500, 5'UTR
cg13959344	6:32901642		
cg08541518	6:69942892	BAI3	Body
cg19509311	6:106429191		
cg00590036	6:158957433	TMEM181	TSS200
cg07955995	7:130419159	KLF14	TSS1500
cg24681895	8:145743681	RECQL4, LRRC14	TSS1500, 5'UTR
cg10217503	12:65153209	GNS	5'UTR, 1st exon
cg22171539	12:81107990		
cg11082362	14:36003181	INSM2	TSS200

cg21801378*	15:72612125	BRUNOL6	1st exon
cg06279276	16:67184164	B3GNT9	Body
cg24668364	17:16284324	UBB	TSS200
cg22361181	17:40171740	NKIRAS2	TSS1500, 5'UTR
cg16969368	17:57642752	DHX40	TSS200
cg17243289	18:45458021	SMAD2	TSS1500
cg16665444	18:76828655	ATP9B	TSS1500
cg02997982	19:41082291	SHKBP1, SPTBN4	TSS1500, 3'UTR

293

Discussion

In this study, we present newly generated genome-wide DNA methylation data from adult human bones spanning a nearly 4 decade age range. We incorporate additional DNA methylation array data derived from living and deceased donors, resulting in a combined dataset that spans a total age range of over 6 decades, which we use to conduct the first comprehensive analysis of patterns of epigenetic aging in adult human bone tissue. We show that a previously published epigenetic age predictor generates reasonably accurate estimates of chronological age based on DNA methylation data from 353 CpG sites (RMSE 7.4) (Horvath 2013).

Surprisingly, we achieved more accurate estimates of chronological age using the Horvath algorithm on the GSE64490 and GSE64491 datasets than the original publication (RMSE of 6.0 years rather than ~8.1 years) (Horvath et al., 2015). This may be due to differences in processing the raw DNA methylation signal data. One major difference is our implementation of the beta mixture quantile dilation (BMIQ) normalization method, which corrects for technical differences between probes measured with the Type I and Type II Illumina chemistry, on all probes in the dataset (Teschendorff et al., 2013). By contrast, Horvath et al. uses a custom script to normalize data, which is based on the BMIQ method but uses a 'gold standard' reference panel of Type II probes (Horvath, 2013; Horvath et al., 2015). There may be additional differences in our processing pipelines beyond this normalization step, but it is nonetheless noteworthy that such significant variation in overall accuracy can result from such differences.

Relative to the best implementation of the Horvath model, I demonstrate that even more accurate estimates of chronological age can be generated for human bone from nearly 10 times fewer sites. There are two likely reasons for this improvement. The first is that the original Horvath model was only trained on CpG sites that were present on an earlier Illumina DNA methylation array, which assayed 27 thousand sites (Horvath 2013). This excluded any sites present on the more comprehensive 450k array, many of which were reported to be excellent potential predictors of age. For example, it was demonstrated that DNA methylation at the gene ELOVL2, and in particular the CpG site cg16867657, showed a strong and precise relationship with age (Garagnani et al., 2012). This association was confirmed in subsequent

studies, which further supported its utility for estimating chronological age in humans with potential forensic applications (Hannum et al., 2013; Johansson et al., 2013; Naue et al., 2017; Spólnicka et al., 2018; Zbieć-Piekarska et al., 2015a). By training our predictor on data from age-associated CpG sites identified from 450k array data, we were able to achieve accurate results using fewer and, arguably, better markers of chronological age.

The second reason for improved accuracy is our focus on a single tissue rather than the Horvath model's focus on multiple tissues. It is well known that genomic patterns of DNA methylation differ broadly across tissue types; in fact, DNA methylation is an important mechanism by which tissue identity is established during development (Lokk et al., 2014; Rakyan et al., 2008). That these tissue-specific differences intersect with changes in DNA methylation with age is also well established (Dmitrijeva et al., 2018; Hannum et al., 2013; Maegawa et al., 2010; Slieker et al., 2018). It is therefore unsurprising that it would be challenging to develop a predictor of age that is equally accurate on all human tissue types. In fact, the Horvath model has been used to argue that different tissues 'age' at different rates based on the consistent deviations from a linear model relating chronological age to the predicted age (Horvath et al., 2015, 2014).

It is important to note here a difference in the motivations behind the Horvath model and any model intended for forensic applications, including the one presented here. The Horvath model is primarily used as a measure of a conceptual 'biological', not chronological, age, which reflects individual functional capacity and overall health rather than simply the number of years lived. The 37 bone clock CpGs identified here may therefore be best suited for forensic applications, and not for estimating health status.

It is interesting to note that one of the significant results of the enrichment analysis was the gene ELOVL2. Two of 37 CpG sites selected by lasso regression, the aforementioned cg16867657 as well as cg23606718, were annotated to this gene. This supports the idea that the gene ELOVL2 is a uniquely useful predictor of chronological age, as it is significantly associated with age across multiple tissue types, including blood, saliva, brain, buccal cells, liver, fat, breast, kidney, lung, teeth, and now, bone, as well as across diverse populations (Bekaert et al., 2015; Giuliani et al., 2016; Gopalan et al., 2017; Hannum et al., 2013; Johansson et al., 2013;

Slieker et al., 2018). However, it is still unclear if the specific relationship between DNA methylation level and age (i.e., the 'slope' and intercept' of the linear model) is consistent across all these tissue types.

The second significant enrichment category identified here was the presence of the AAGCACA motif in the 3' UTR. Genes that bear this motif are putative targets of negative regulation by the miR-218 microRNA, which carries the complementary sequence (Subramanian et al., 2005). It has been shown that miR-218 is upregulated during osteoblast differentiation, driving bone differentiation via a positive feedback loop involving the Wnt pathway (Hassan et al., 2012). Interestingly, while miR-218 has been shown to have tumor-suppressing activity in multiple tissue types, it also promotes metastasis of breast cancer to bone by mimicking this molecular signature of bone differentiation (Alajez et al., 2011; Hassan et al., 2012; Liu et al., 2018; Tatarano et al., 2011; Venkataraman et al., 2013; Yang et al., 2017). While it is unclear if the enrichment of miR-218 targets among the bone clock CpGs is meaningful, it is nevertheless tempting to speculate that it suggests a bone-specific characteristic of our predictive model.

A significant limitation of this study is the age range of individuals available for training the model. While the datasets altogether provided a cross-section of 63 years of adult human lifespan, it is not clear if our bone clock can accurately estimate the age of younger adults. In an attempt to improve age-association detection power by increasing the sample size and the age range surveyed, we also assayed 13 forensic samples on the EPIC methylation array (see *Methods*). Unfortunately, none of these passed post-assay quality control metrics and therefore could not be reliably analyzed alongside the other samples. It is likely that the DNA in these samples was already too degraded for quantitative measures of DNA methylation to be recovered after a few years of exposure to the elements and taphonomic processes. A common type of DNA damage occurs when cytosines are spontaneously degraded into thymines if they are methylated or uracils if they are unmethylated. Bisulphite treatment, which precedes most DNA methylation assay techniques, also converts unmethylated cytosines to uracils that are later read as thymines, but does not affect methylated cytosines; the attached methyl group 'protects' those cytosines from being mutated. DNA methylation levels are subsequently measured from the difference between the cytosines and thymines at a given CpG site.

Therefore, post-mortem cytosine damage will generally make methylated cytosines appear unmethylated, a phenomenon that is the likely explanation for the large difference observed between the median methylated and unmethylated signals in the forensic samples (Figure 1).

The poor quality of our forensic DNA samples does not negate the utility of bone-specific DNA methylation-based age predictor. It does, however, highlight several practical considerations related to the application of any method that relies on good-quality DNA, including preservation and skeletal element choice . These issues have started to be investigated in the context of ancient DNA, where there is significant interest in understanding the DNA methylation profiles of individuals at different points in the past (Gokhman et al., 2017, 2014; Llamas et al., 2012; Pedersen et al., 2014; Seguin-Orlando et al., 2015; Smith et al., 2015). Studies have shown that it is possible to recover accurate measurements of DNA methylation at individual CpG site level even for samples that are thousands of years old (Llamas et al., 2012; Smith et al., 2015). However, the success of such bisulfite-based DNA methylation assays depends on the quality and preservation of the input DNA (Seguin-Orlando et al., 2015). Therefore, bone clock developed here may have substantial utility for forensic investigations when used in the appropriate contexts.

The forensic samples in the present study may have been from individuals that were particularly poorly preserved, but additionally, the skeletal element sampled, the intercondylar fossa of the femur, is not ideal for the recovery of DNA. Ancient DNA studies have shown that the petrous portion of the temporal bone is a good source of DNA that is relatively resistant to contamination and degradation (Gamba et al., 2014; Pinhasi et al., 2015). It is, however, difficult to access without significant destruction of the skull, which was permitted for the preserved samples but not for those sourced from the forensic collection. In ancient DNA studies, a sample's collagen content is usually measured first before deciding if sequencing should be done, as this is a good indicator of preservation and DNA quality (Ovchinnikov et al., 2000). This may also be a worthwhile step to incorporate into a forensic investigation workflow when deciding which aging method is most appropriate for a given case.

In this study, we show that chronological age can be accurately estimated from bone-derived DNA from human adults. This model represents a promising molecular method that

410 may be useful for building biological profiles of unknown individuals in forensic cases. Future
411 research to focus on further refining the bone clock CpG set may allow for the development of
412 more precise and, importantly, more cost-effective methods of aging individuals' skeletal
413 remains using DNA methylation markers.
414

Acknowledgements

We would like to thank Daniel Wescott, Randall Susman, and Danny Soto for generously granting access to their respective collections of human remains. We would also like to thank Sjur Reppe for providing access to his bone DNA methylation dataset. Research funding and support for SG was provided by a National Institute of Justice Graduate Research Fellowship (2016-DN-BX-0011). JG was supported by a grant from the Undergraduate Research and Creative Activities summer program (URECA, Stony Brook University).

References

Alajez, N.M., Lenarduzzi, M., Ito, E., Hui, A.B.Y., Shi, W., Bruce, J., Yue, S., Huang, S.H., Xu, W., Waldron, J., O'Sullivan, B., Liu, F.F., 2011. miR-218 suppresses nasopharyngeal cancer progression through downregulation of survivin and the SLIT2-ROBO1 pathway. Cancer Res. 71, 2381–2391.

Aryee, M.J., Jaffe, A.E., Corrada-Bravo, H., Ladd-Acosta, C., Feinberg, A.P., Hansen, K.D., Irizarry, R.A., 2014. Minfi: a flexible and comprehensive Bioconductor package for the analysis of Infinium DNA methylation microarrays. Bioinformatics 30, 1363–1369.

Bekaert, B., Kamalandua, A., Zapico, S.C., Voorde, W. Van De, Decorte, R., 2015. Improved age determination of blood and teeth samples using a selected set of DNA methylation markers. Epigenetics 10, 922–930.

Chen, Y.A., Lemire, M., Choufani, S., Butcher, D.T., Grafodatskaya, D., Zanke, B.W., Gallinger, S., Hudson, T.J., Weksberg, R., 2013. Discovery of cross-reactive probes and polymorphic CpGs in the Illumina Infinium HumanMethylation450 microarray. Epigenetics 8, 203–209.

Cunha, E., Baccino, E., Martrille, L., Ramsthaler, F., Prieto, J., Schuliar, Y., Lynnerup, N., Cattaneo, C., 2009. The problem of aging human remains and living individuals: a review. Forensic Sci. Int. 193, 1–13.

Davis, S., Du, P., Bilke, S., Triche, T., Bootwalla, M., 2015. methylumi: Handle Illumina methylation data.

Dmitrijeva, M., Ossowski, S., Serrano, L., Schaefer, M.H., 2018. Tissue-specific DNA methylation loss during ageing and carcinogenesis is linked to chromosome structure, replication timing and cell division rates. Nucleic Acids Res. 46, 7022–7039.

Du, P., Kibbe, W.A., Lin, S.M., 2008. lumi: a pipeline for processing Illumina microarray. Bioinformatics 24, 1547–1548.

Franklin, D., 2010. Forensic age estimation in human skeletal remains: current concepts and future directions. Leg. Med. 12, 1–7.

Friedman, J., Hastie, T., Tibshirani, R., 2010. Regularization paths for generalized linear models via coordinate descent. J. Stat. Softw. 33, 1–22.

Gamba, C., Jones, E.R., Teasdale, M.D., McLaughlin, R.L., Gonzalez-Fortes, G., Mattiangeli, V., Domboróczki, L., Kővári, I., Pap, I., Anders, A., Whittle, A., Dani, J., Raczky, P., Higham, T.F.G., Hofreiter, M., Bradley, D.G., Pinhasi, R., 2014. Genome flux and stasis in a five millennium transect of European prehistory. Nat. Commun. 5, 5257.

Garagnani, P., Bacalini, M.G., Pirazzini, C., Gori, D., Giuliani, C., Mari, D., Di Blasio, A.M., Gentilini, D., Vitale, G., Collino, S., Rezzi, S., Castellani, G., Capri, M., Salvioli, S., Franceschi, C., 2012. Methylation of ELOVL2 gene as a new epigenetic marker of age. Aging Cell 11, 1132–1134.

Gibbon, V.E., Penny, C.B., Štrkalj, G., Ruff, P., 2009. Brief communication: minimally invasive bone sampling method for DNA analysis. Am. J. Phys. Anthropol. 139, 596–599.

Giuliani, C., Cilli, E., Bacalini, M.G., Pirazzini, C., Sazzini, M., Gruppioni, G., Franceschi, C., Garagnani, P., Luiselli, D., 2016. Inferring chronological age from DNA methylation patterns of human teeth. Am. J. Phys. Anthropol. 159, 585–595.

Gokhman, D., Lavi, E., Prüfer, K., Fraga, M.F., Riancho, J.A., Kelso, J., Pääbo, S., Meshorer, E., Carmel, L., 2014. Reconstructing the DNA methylation maps of the Neandertal and the Denisovan. Science. 344, 523–527.

Gokhman, D., Malul, A., Carmel, L., 2017. Inferring past environments from ancient epigenomes. Mol. Biol. Evol. 34, 2429–2438.

Gopalan, S., Carja, O., Fagny, M., Patin, E., Myrick, J.W., McEwen, L.M., Mah, S.M., Kobor, M.S., Froment, A., Feldman, M.W., Quintana-Murci, L., Henn, B.M., 2017. Trends in DNA methylation with age replicate across diverse human populations. Genetics 206, 1659–1674.

Hannum, G., Guinney, J., Zhao, L., Zhang, L., Hughes, G., Sadda, S., Klotzle, B., Bibikova, M., Fan, J.-B., Gao, Y., Deconde, R., Chen, M., Rajapakse, I., Friend, S., Ideker, T., Zhang, K., 2013. Genome-wide methylation profiles reveal quantitative views of human aging rates. Mol. Cell 49, 359–367.

Hassan, M.Q., Maeda, Y., Taipaleenmaki, H., Zhang, W., Jafferji, M., Gordon, J.A.R., Li, Z., Croce, C.M., van Wijnen, A.J., Stein, J.L., Stein, G.S., Lian, J.B., 2012. miR-218 directs a Wnt

signaling circuit to promote differentiation of osteoblasts and osteomimicry of metastatic cancer cells. J. Biol. Chem. 287, 42084–42092.

Hong, S.R., Jung, S.-E., Lee, E.H., Shin, K.-J., Yang, W.I., Lee, H.Y., 2017. DNA methylation-based age prediction from saliva: high age predictability by combination of 7 CpG markers. Forensic Sci. Int. Genet. 29, 118–125.

Horvath, S., 2013. DNA methylation age of human tissues and cell types. Genome Biol. 14, R115.

Horvath, S., Erhart, W., Brosch, M., Ammerpohl, O., Schönfels, W. von, Ahrens, M., Heits, N., Bell, J.T., Tsai, P.-C., Spector, T.D., Deloukas, P., Siebert, R., Sipos, B., Becker, T., Röcken, C., Schafmayer, C., Hampe, J., 2014. Obesity accelerates epigenetic aging of human liver. Proc. Natl. Acad. Sci. 201412759.

Horvath, S., Mah, V., Lu, A.T., Woo, J.S., Choi, O.-W., Jasinska, A.J., Riancho, J.A., Tung, S., Coles, N.S., Braun, J., Vinters, H. V, Coles, L.S., 2015. The cerebellum ages slowly according to the epigenetic clock. Aging 7, 294–305.

Johansson, A., Enroth, S., Gyllensten, U., 2013. Continuous aging of the human DNA methylome throughout the human lifespan. PLoS One 8, e67378.

Lee, H.Y., Jung, S.E., Oh, Y.N., Choi, A., Yang, W.I., Shin, K.J., 2015. Epigenetic age signatures in the forensically relevant body fluid of semen: a preliminary study. Forensic Sci. Int. Genet. 19, 28–34.

Liu, X., Cao, M., Palomares, M., Wu, X., Li, A., Yan, W., Fong, M.Y., Chan, W.-C., Wang, S.E., 2018. Metastatic breast cancer cells overexpress and secrete miR-218 to regulate type I collagen deposition by osteoblasts. Breast Cancer Res. 20, 127.

Llamas, B., Holland, M.L., Chen, K., Cropley, J.E., Cooper, A., Suter, C.M., 2012. High-resolution analysis of cytosine methylation in ancient DNA. PLoS One 7, e30226.

Lokk, L., Modhukur, V., Rajashekar, B., Märtens, K., Mägi, R., Kolde, R., Koltšina, M., Nilsson, T., Vilo, J., Salumets, A., Tõnisson, N., 2014. DNA methylome profiling of human tissues identifies global and tissue-specific methylation patterns. Genome Biol. 15, r54.

505 Maegawa, S., Hinkal, G., Kim, H.S., Shen, L., Zhang, L., Zhang, J., Zhang, N., Liang, S., Donehower,
506 L.A., Issa, J.-P.J., 2010. Widespread and tissue specific age-related DNA methylation
507 changes in mice. Genome Res. 20, 332–340.
508 McLean, C.Y., Bristor, D., Hiller, M., Clarke, S.L., Schaar, B.T., Lowe, C.B., Wenger, A.M.,
509 Bejerano, G., 2010. GREAT improves functional interpretation of cis-regulatory regions.
510 Nat. Biotechnol. 28, 495–501.
511 Meissner, C., Ritz-Timme, S., 2010. Molecular pathology and age estimation. Forensic Sci. Int.
512 203, 34–43.
513 Naue, J., Hoefsloot, H.C.J., Mook, O.R.F., Rijlaarsdam-Hoekstra, L., van der Zwalm, M.C.H.,
514 Henneman, P., Kloosterman, A.D., Verschure, P.J., 2017. Chronological age prediction
515 based on DNA methylation: massive parallel sequencing and random forest regression.
516 Forensic Sci. Int. Genet. 31, 19–28.
517 Ohtani, S., Yamamoto, T., 2010. Age estimation by amino acid racemization in human teeth. J.
518 Forensic Sci. 55, 1630–1633.
519 Ovchinnikov, I. V., Götherström, A., Romanova, G.P., Kharitonov, V.M., Lidén, K., Goodwin, W.,
520 2000. Molecular analysis of Neanderthal DNA from the northern Caucasus. Nature 404,
521 490–493.
522 Pedersen, J.S., Valen, E., Velazquez, A.M.V., Parker, B.J., Rasmussen, M., Lindgreen, S., Lilje, B.,
523 Tobin, D.J., Kelly, T.K., Vang, S., Andersson, R., Jones, P.A., Hoover, C.A., Tikhonov, A.,
524 Prokhortchouk, E., Rubin, E.M., Sandelin, A., Gilbert, M.T.P., Krogh, A., Willerslev, E.,
525 Orlando, L., 2014. Genome-wide nucleosome map and cytosine methylation levels of an
526 ancient human genome. Genome Res. 24, 454–466.
527 Pidsley, R., Wong, C.C.Y., Volta, M., Lunnon, K., Mill, J., Schalkwyk, L.C., 2013. A data-driven
528 approach to preprocessing Illumina 450K methylation array data. BMC Genomics 14, 293.
529 Pidsley, R., Zotenko, E., Peters, T.J., Lawrence, M.G., Risbridger, G.P., Molloy, P., Van Djik, S.,
530 Muhlhausler, B., Stirzaker, C., Clark, S.J., 2016. Critical evaluation of the Illumina
531 MethylationEPIC BeadChip microarray for whole-genome DNA methylation profiling.
532 Genome Biol. 17, 208.

Pinhasi, R., Fernandes, D., Sirak, K., Novak, M., Connell, S., Alpaslan-Roodenberg, S., Gerritsen, F., Moiseyev, V., Gromov, A., Raczky, P., Anders, A., Pietrusewsky, M., Rollefson, G., Jovanovic, M., Trinhhoang, H., Bar-Oz, G., Oxenham, M., Matsumura, H., Hofreiter, M., 2015. Optimal ancient DNA yields from the inner ear part of the human petrous bone. PLoS One 10, e0129102.

Rakyan, V.K., Down, T.A., Thorne, N.P., Flicek, P., Kulesha, E., Gräf, S., Tomazou, E.M., Bäckdahl, L., Johnson, N., Herberth, M., Howe, K.L., Jackson, D.K., Miretti, M.M., Fiegler, H., Marioni, J.C., Birney, E., Hubbard, T.J.P., Carter, N.P., Tavaré, S., Beck, S., 2008. An integrated resource for genome-wide identification and analysis of human tissue-specific differentially methylated regions (tDMRs). Genome Res. 18, 1518–1529.

Reppe, S., Lien, T.G., Hsu, Y.-H., Gautvik, V.T., Olstad, O.K., Yu, R., Bakke, H.G., Lyle, R., Kringen, M.K., Glad, I.K., Gautvik, K.M., 2017. Distinct DNA methylation profiles in bone and blood of osteoporotic and healthy postmenopausal women. Epigenetics 12, 674–687.

Rohatgi, A., 2018. WebPlotDigitizer.

Seguin-Orlando, A., Gamba, C., Der Sarkissian, C., Ermini, L., Louvel, G., Boulygina, E., Sokolov, A., Nedoluzhko, A., Lorenzen, E.D., Lopez, P., McDonald, H.G., Scott, E., Tikhonov, A., Stafford, T.W., Alfarhan, A.H., Alquraishi, S.A., Al-Rasheid, K.A.S., Shapiro, B., Willerslev, E., Prokhortchouk, E., Orlando, L., 2015. Pros and cons of methylation-based enrichment methods for ancient DNA. Sci. Rep. 5, 11826.

Slieker, R.C., Relton, C.L., Gaunt, T.R., Slagboom, P.E., Heijmans, B.T., 2018. Age-related DNA methylation changes are tissue-specific with ELOVL2 promoter methylation as exception. Epigenetics and Chromatin 11, 25.

Smith, R.W.A., Monroe, C., Bolnick, D.A., 2015. Detection of cytosine methylation in ancient DNA from five Native American populations using bisulfite sequencing. PLoS One 10, e0125344.

Spólnicka, M., Pośpiech, E., Pepłońska, B., Zbieć-Piekarska, R., Makowska, Ż., Pięta, A., Karłowska-Pik, J., Ziemkiewicz, B., Wężyk, M., Gasperowicz, P., Bednarczuk, T., Barcikowska, M., Żekanowski, C., Płoski, R., Branicki, W., 2018. DNA methylation in

561 ELOVL2 and C1orf132 correctly predicted chronological age of individuals from three
562 disease groups. Int. J. Legal Med. 132, 1–11.
563 Subramanian, A., Tamayo, P., Mootha, V.K., Mukherjee, S., Ebert, B.L., Gillette, M.A., Paulovich,
564 A., Pomeroy, S.L., Golub, T.R., Lander, E.S., Mesirov, J.P., 2005. Gene set enrichment
565 analysis: a knowledge-based approach for interpreting genome-wide expression profiles.
566 Proc. Natl. Acad. Sci. 102, 15545–15550.
567 Tatarano, S., Chiyomaru, T., Kawakami, K., Enokida, H., Yoshino, H., Hidaka, H., Yamasaki, T.,
568 Kawahara, K., Nishiyama, K., Seki, N., Nakagawa, M., 2011. miR-218 on the genomic loss
569 region of chromosome 4p15.31 functions as a tumor suppressor in bladder cancer. Int. J.
570 Oncol. 39, 13–21.
571 Teschendorff, A.E., Marabita, F., Lechner, M., Bartlett, T., Tegner, J., Gomez-Cabrero, D., Beck,
572 S., 2013. A beta-mixture quantile normalization method for correcting probe design bias
573 in Illumina Infinium 450 k DNA methylation data. Bioinformatics 29, 189–196.
574 Venkataraman, S., Birks, D.K., Balakrishnan, I., Alimova, I., Harris, P.S., Patel, P.R., Handler, M.H.,
575 Dubuc, A., Taylor, M.D., Foreman, N.K., Vibhakar, R., 2013. MicroRNA 218 acts as a tumor
576 suppressor by targeting multiple cancer phenotype-associated genes in medulloblastoma.
577 J. Biol. Chem. 288, 1918–1928.
578 Vidaki, A., Ballard, D., Aliferi, A., Miller, T.H., Barron, L.P., Syndercombe Court, D., 2017. DNA
579 methylation-based forensic age prediction using artificial neural networks and next
580 generation sequencing. Forensic Sci. Int. Genet. 28, 225–236.
581 Yang, Y., Ding, L., Hu, Q., Xia, J., Sun, J., Wang, X., Xiong, H., Gurbani, D., Li, L., Liu, Y., Liu, A.,
582 2017. MicroRNA-218 functions as a tumor suppressor in lung cancer by targeting IL-
583 6/STAT3 and negatively correlates with poor prognosis. Mol. Cancer 16, 141.
584 Yi, S.H., Xu, L.C., Mei, K., Yang, R.Z., Huang, D.X., 2014. Isolation and identification of age-related
585 DNA methylation markers for forensic age-prediction. Forensic Sci. Int. Genet. 11, 117–
586 125.
587 Zbieć-Piekarska, R., Spólnicka, M., Kupiec, T., Makowska, Ż., Spas, A., Parys-Proszek, A.,
588 Kucharczyk, K., Płoski, R., Branicki, W., 2015a. Examination of DNA methylation status of

the ELOVL2 marker may be useful for human age prediction in forensic science. Forensic Sci. Int. Genet. 14, 161–167.

Zbieć-Piekarska, R., Spólnicka, M., Kupiec, T., Parys-Proszek, A., Makowska, Ż., Pałeczka, A., Kucharczyk, K., Płoski, R., Branicki, W., 2015b. Development of a forensically useful age prediction method based on DNA methylation analysis. Forensic Sci. Int. Genet. 17, 173–179.